PHYSOR 2004 -The Physics of Fuel Cycles and Advanced Nuclear Systems: Global Developments
Chicago, Illinois, April 25-29, 2004, on CD-ROM, American Nuclear Society, Lagrange Park, IL. (2004)

TORT Solutions to the Three-Dimensional MOX Neutron Transport Benchmark Problem, 3-D Extension C5G7 MOX

Jesse J Klingensmith[1*], Yousry Y. Azmy[2], Jess C. Gehin[3], and Roberto Orsi[4]
[1] *Pennsylvania State Univeristy, 138 Reber Building, University Park, PA 16802*
[2] *Pennsylvania State Univeristy, 229 Reber Building, University Park, PA 16802*
[3] *Oak Ridge National Laboratory, P.O. Box 2008, MS 6363, Oak Ridge, TN 37381*
[4] *ENEA FIS-NUC, Via Martiri di Monte Sole, 4, 40129 Bologna, Italy*

This paper details the results for the OECD/NEA C5G7MOX benchmark obtained using the DOORS code TORT. This benchmark is intended to test modern radiation transport codes' abilities to handle three-dimensional problems with spatial heterogeneity. The problem consists of a four-assembly UO_2 and MOX fuel reflected reactor core in which control rods are inserted to three distinct levels, *Unrodded, Rodded A*, and *Rodded B*. A Monte Carlo reference solution was provided with the benchmark. Effective multiplication factor results varied from 0.06% error for the *Unrodded* case to 0.17% and 0.67% for the *Rodded A* and *Rodded B* cases, respectively. The pin power results followed a similar trend. Varying the meshing and angular quadrature refinement did change the results, but not sufficiently to justify the additional computation time.

***KEYWORDS**: Transport theory, MOX core calculations, benchmark, TORT, three-dimensional*

1. Introduction

The OECD/NEA Experts Group on Three-Dimensional Radiation Transport has previously conducted a benchmark exercise in which a small core configuration consisting of UO_2 and MOX PWR fuel assemblies were modeled in three-dimensions without spatial homogenizations [1]. This benchmark proved to be a good test for radiation transport codes modeling the local details of the fuel rod in two dimensions, but was relatively uniform in the axial direction. A three dimensional extension of the C5G7 MOX benchmark was proposed as a more realistic test of neutron transport methods' ability to accurately model three-dimensional nuclear reactor configurations. This was done by introducing more spatial heterogeneity in the third dimension, i.e. along the z-axis, in the form of control rods [2]. In addition to the problem geometry, which will be detailed later, the material composition, abbreviated (seven energy groups) cross-section library, and Monte Carlo reference solution were provided for comparison with deterministic methods' results.

* Corresponding author, E-mail: jxk390@psu.edu

The results detailed in this paper were obtained using the DOORS (Discrete Ordinates Oak Ridge System) codes, in particular TORT (Three-Dimensional Discrete Ordinates Neutron/Photon Transport Code) [3]. The DOORS system was developed at the Oak Ridge National Laboratory for use in radiation transport for shielding applications and for modeling nuclear systems. The computers used in the study are Linux-based PCs with dual 2 GHz processors and 512 MB of RAM. The geometry inputs and output visualization was done using the BOT3P code system [4].

2. Geometry and Material Specification

The changes to the benchmark problem to add heterogeneity are detailed as follows. The overall height of the problem geometry has been reduced from 192.78 cm to 64.26 cm. Additionally, the control rod guide tubes are present in the upper axial reflector. The introduction of control rods to the problem geometry necessitates using a cross section set for the guide tube/control rod geometry [2].

Included within the benchmark extension are three separate core configurations corresponding to three different levels of control rod insertion. The first is the *Unrodded* case, in which the control elements are present in the upper reflector of all four fuel assemblies included in the model. Figure 1 shows an axial slice of the reactor core with no control elements inserted. The dark blue indicates the location of the guide tubes for control rod insertion. The red pins represent UO_2 fuel rods. The assembly located at the origin of the *x-y* axis will be referred to as the *inner* UO_2 assembly. Conversely, the other UO_2 assembly will be referred to as the *outer* UO_2 assembly. The eighth-core symmetry of the problem allows the MOX assemblies to be treated as identical.

The *Rodded A* case is identical to the *Unrodded* case except with the insertion of control elements into the inner UO_2 assembly one-third the length of the core. Figure 3 shows the sections of the core in which the control elements have been inserted shaded in grey for the *Rodded A* case. Note that Fig. 2 shows the relative locations of radial slices A-A and B-B. Figure 4 shows the control element insertion for the *Rodded B* case, which corresponds to two-thirds insertion in the center UO_2 assembly and one-third insertion in the MOX assemblies. [2]

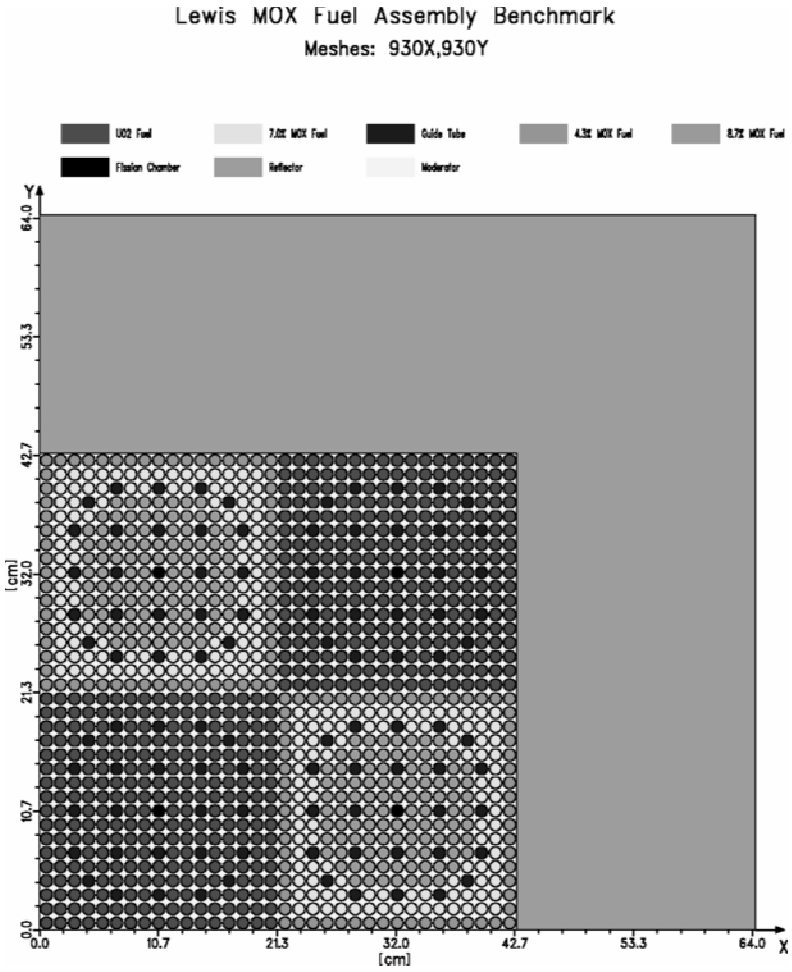

Fig. 1: Axial Slice Core Geometry for MOX Benchmark, C5G7

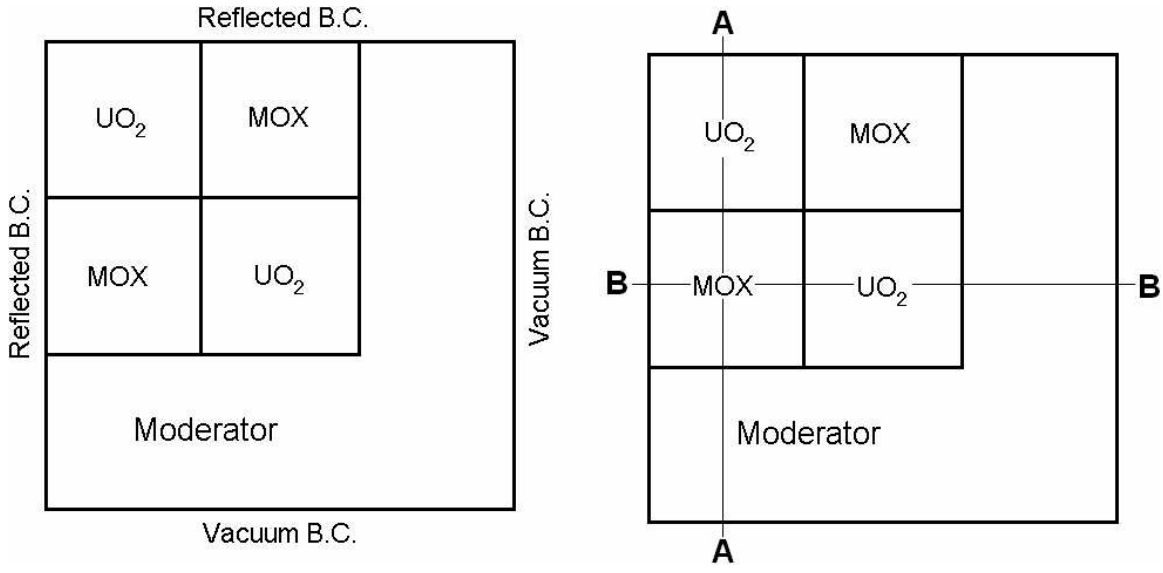

Fig. 2: Simplified Core Layout Showing Radial Slices and Boundary Conditions

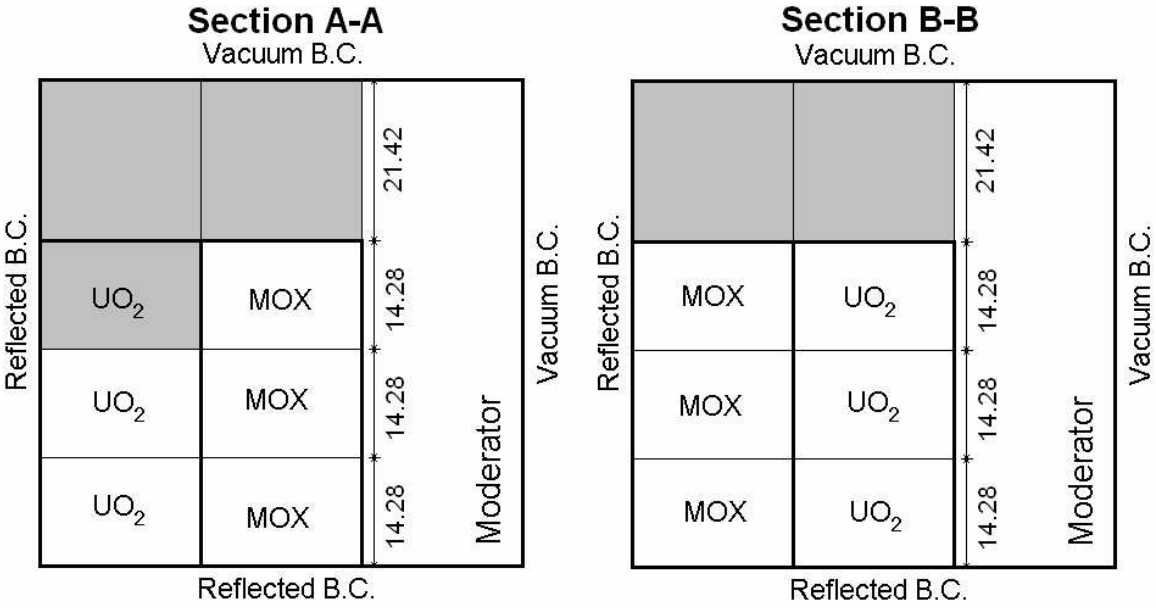

Fig. 3: Levels of Control Rod Insertion for *Rodded A* Case

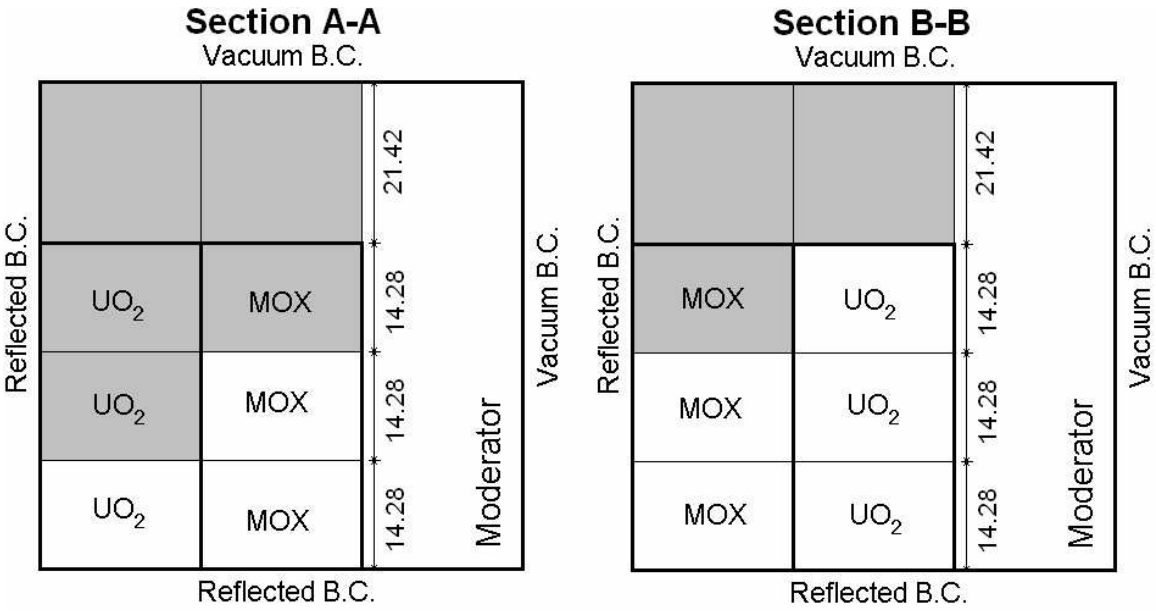

Fig. 4: Levels of Control Rod Insertion for *Rodded B* Case

3. Mesh Refinement Studies

Two separate types of mesh refinement were attempted to determine the effect on the accuracy of the effective multiplication factor and pin powers. For the purposes of this report, the variation of the meshing in the *x*- and *y*-coordinate directions will be referred to as the radial mesh refinement, and the variation along the *z*-coordinate direction will be referred to as the axial mesh. For all variations of mesh refinement, the volume of all bodies is exactly conserved by the mesh generation capability of the BOT3P code system.

Figure 5 shows the effect of increasing radial mesh refinement on a single fuel pin cell. For the simplest case, the pin cell is divided into a five-by-five mesh, in which the fuel pin, in this mesh geometry, takes on a cruciform shape. This is the "Kdiv"=1 case ("Kdiv" being a parameter in BOT3P that determines the mesh refinement). The refinement in Fig. 5 is shown to be increasing from left to right, or Kdiv of 1, 2, 4, and 8. The Kdiv=2 case corresponds to a seven-by-seven mesh, the Kdiv=4 to an 11-by-11 mesh, and Kdiv=8 to a 19-by-19 cell mesh. Increasing the value of Kdiv improves the staircase approximation of the curved surface of the fuel rod, but does so at the expense of an increased number of computational cells, and thus a longer computing time.

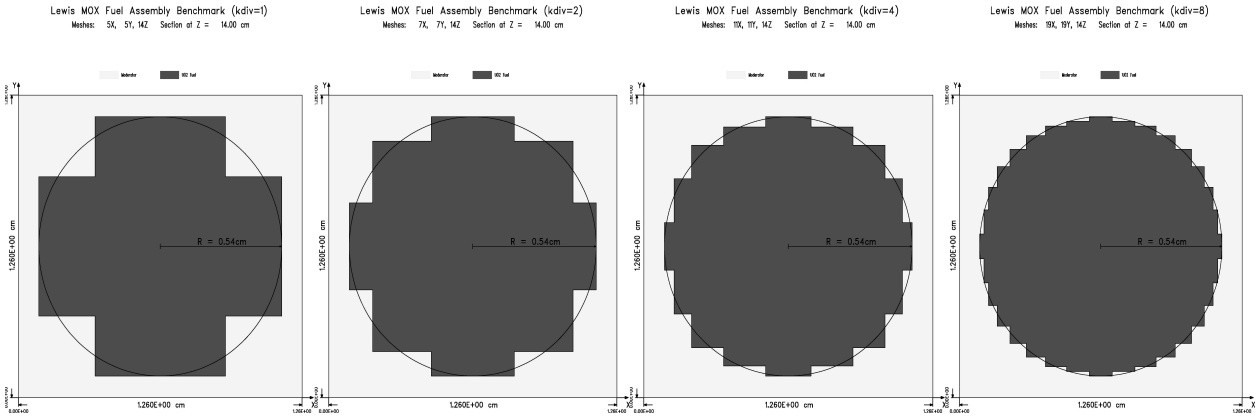

Fig. 5: Effect of Increasing Radial Mesh Refinement Corresponding to Kdiv=1,2,4,8

The axial refinement was also varied to determine the effects on the accuracy of the effective multiplication factor and pin powers. The initial configuration consisted of 14 total computational cells along the *z*-axis, divided into three cells per core slice and five cells in the upper moderator. The alternative primary configuration with axial mesh refinement consisted of 28 cells. This was done by simply splitting each of the previous computational cells into two, thus doubling the total number of cells. Additionally there were several configurations tested that included especially finer meshing at the tips of control elements, though the results of these cases did not show notable improvement over the method of doubling all computational cells.

4. Angular Quadrature Studies

The two different angular quadratures employed in this study were the fully-symmetric, S_n, and the Square Legendre-Chebychev (SLC) quadratures, denoted by Q_n.

For both cases, n is the order of the quadrature set. The S_n quadrature provides a perfectly symmetric, hence rotationally invariant, scattering source in the radial plane given the configuration's symmetry. Also, the order of the quadrature is limited by the tendency to produce negative angular weights for quadratures of order greater than 22. The S_6, S_{12}, and S_{16} sets were used in the form that is distributed with the DOORS code system

The Q_n, or Square Legendre-Chebychev (SLC), quadrature sets forsake full symmetry to ensure that the multi-dimensional moments of the angular flux are better conserved. The angular approximations are considered to be separable, using Legendre integrals in the μ–direction and Chebychev integrals in the ϕ-direction. SLC quadratures of orders 6, 8, 10, 12, and 14 were used and the results are described below.

5. Numerical Results

The first results to be presented are the values of the effective multiplication factor for the three cases with varying radial mesh refinement and order of fully symmetric quadrature. The three points along the x-axis correspond to Kdiv values of 1, 2, and 4. The Kdiv equal to eight data points were not all collected due to processing times in excess of one week. The quadrature order was not increased to greater than 16 due to both the long run times and the inherent instability of this quadrature set due to negative flux weights at high orders.

Figure 6 shows the results for the *Unrodded* case. For a fixed value of Kdiv, or radial mesh refinement, increasing the order of the quadrature from S_6 to S_{12} can be seen to decrease the accuracy of the effective multiplication factor. When the order is increased further, from S_{12} to S_{16}, the accuracy increases to a value that is better than that of the S_6 case. This would indicate that higher order quadrature sets could lead to increased accuracy, but these sets are not available. Even if the sets were available, the S_{16} sets required at the least two to three days to compute indicating that higher order sets may not be practical at this point.

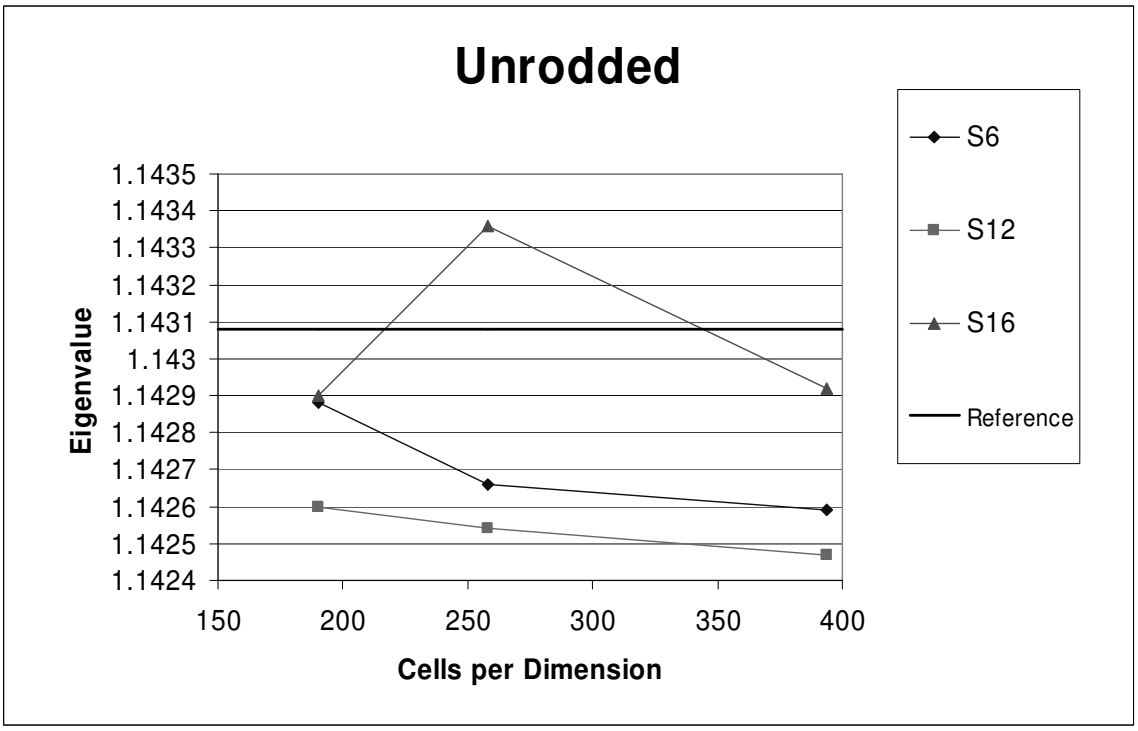

Fig. 6: Effective Multiplication Factor as a function of Radial Mesh and Fully-Symmetrical Quadrature Order for the *Unrodded* Case

The *Rodded A* and *Rodded B* effective multiplication factor results follow the same pattern as the *Unrodded* case, as can be seen below in Figs. 7 and 8.

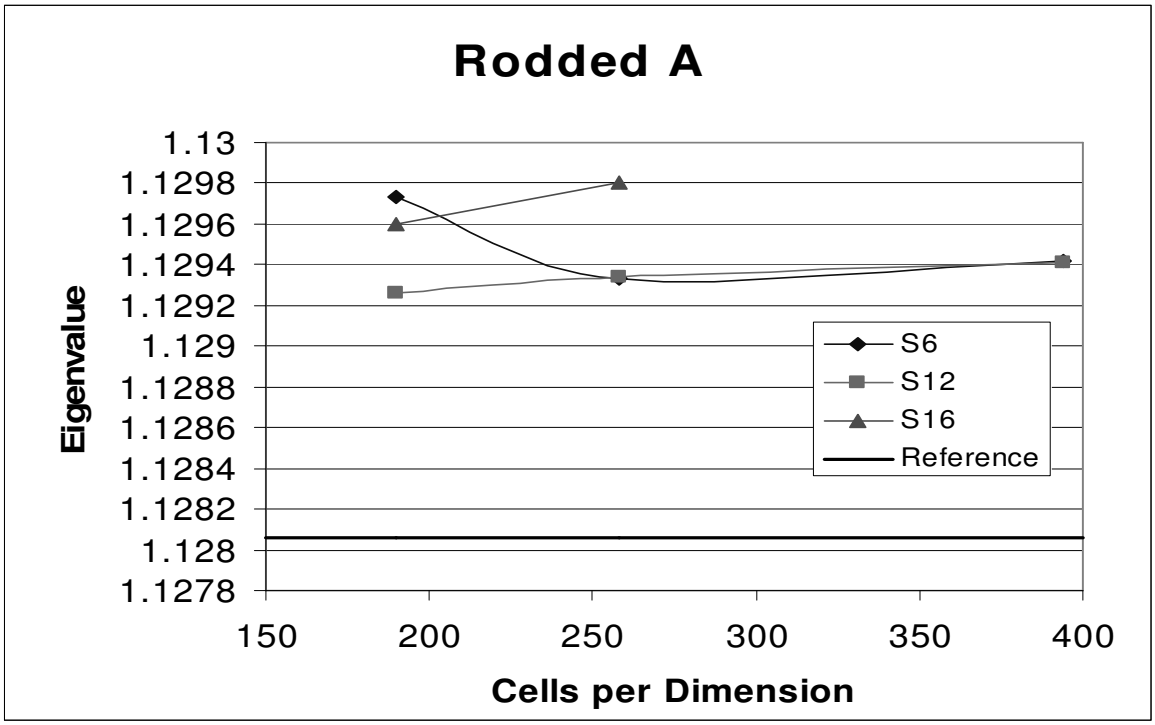

Fig. 7: Effective Multiplication Factor as a function of Radial Mesh and Fully-Symmetrical Quadrature Order for the *Rodded A* Case

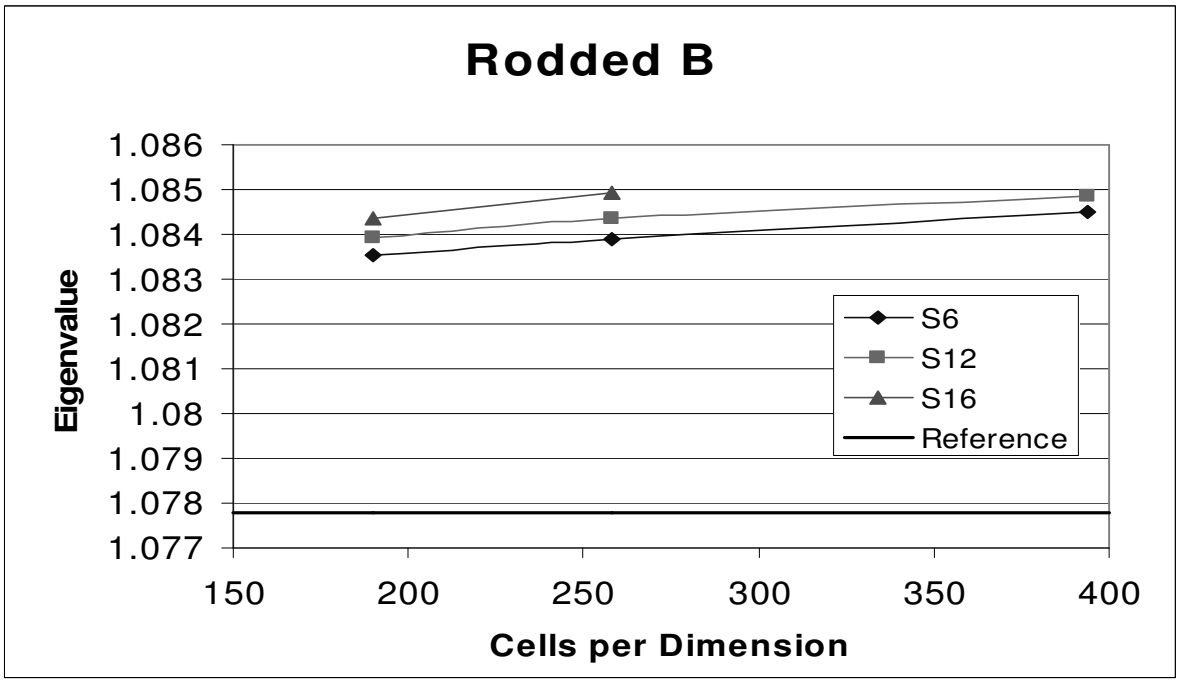

Fig. 8: Effective Multiplication Factor as a function of Radial Mesh and Fully-Symmetrical Quadrature Order for the *Rodded B* Case

In an attempt to increase the maximum number of directions in the quadrature, the SLC quadratures of order 6, 8, 10, 12, and 14 were also attempted. Since increases in radial mesh refinement were not shown to dramatically improve the results, the SLC quadrature work was confined to Kdiv equal to one and two. For comparison, the S_{16} quadrature set contains 320 directions, while the Q_{14}, SLC quadrature order 14, set contains 420 directions. Figure 9 shows the effective multiplication factor as a function of increasing SLC quadrature order and also Kdiv for the *Rodded A* case. It is noteworthy that increasing the quadrature order does not improve the results.

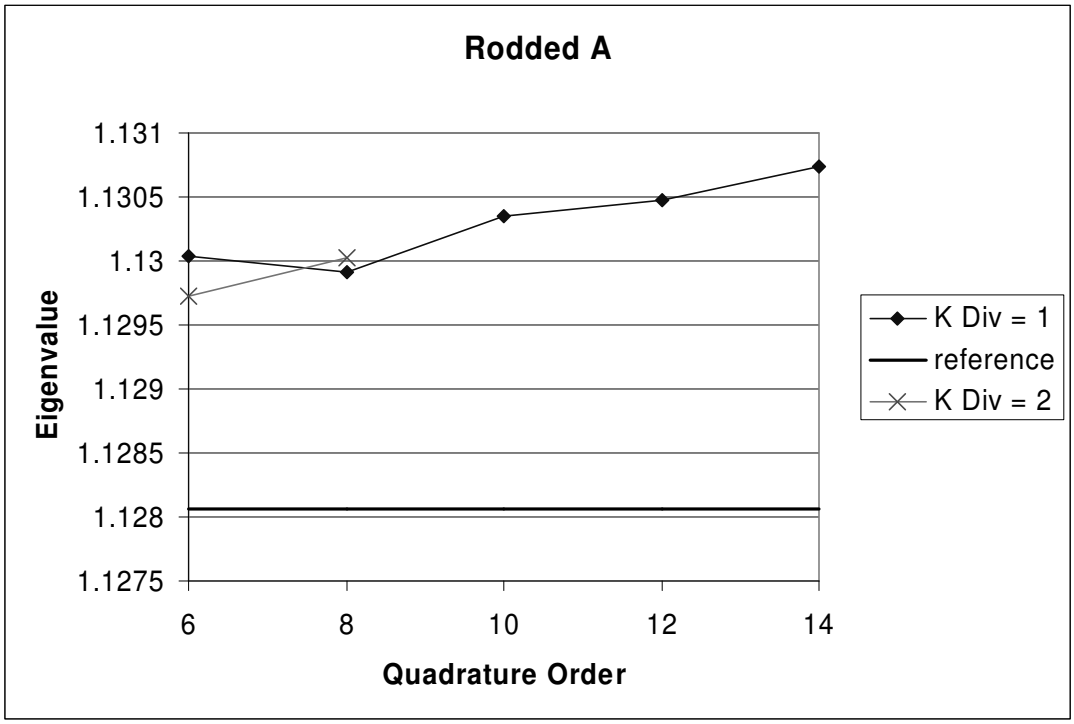

Fig. 9: Effective Multiplication Factor Results for SLC Quadrate, *Rodded A* case

Comparison of the SLC quadrature results with the fully-symmetric quadrature results shows that the difference in percent error compared to the reference is on the order of less than one-hundredth of a percent. This would seem to indicate that the quadrature sets function equally well, or poorly, for this problem. Because of this, the *Unrodded* and *Rodded B* plots are not shown here, though it should be noted that the behavior of the *Rodded A* case is representative of the other two cases.

As to the effect of changing the radial mesh and angular quadrature on the pin power errors, Figs. 10-12 show the results for both quadrature types and Kdiv values of one and two. The three cases were chosen to show the effects of both changing the quadrate set, from S_6 to Q_6, and changing the radial mesh refinement, from Kdiv=1 to Kdiv=2. These low refinements were chosen as to minimize the computational times required. The above results and results not shown here indicate that there is no appreciable

improvement in the accuracy of the results as compared to more computationally intensive simulations with higher refinements.

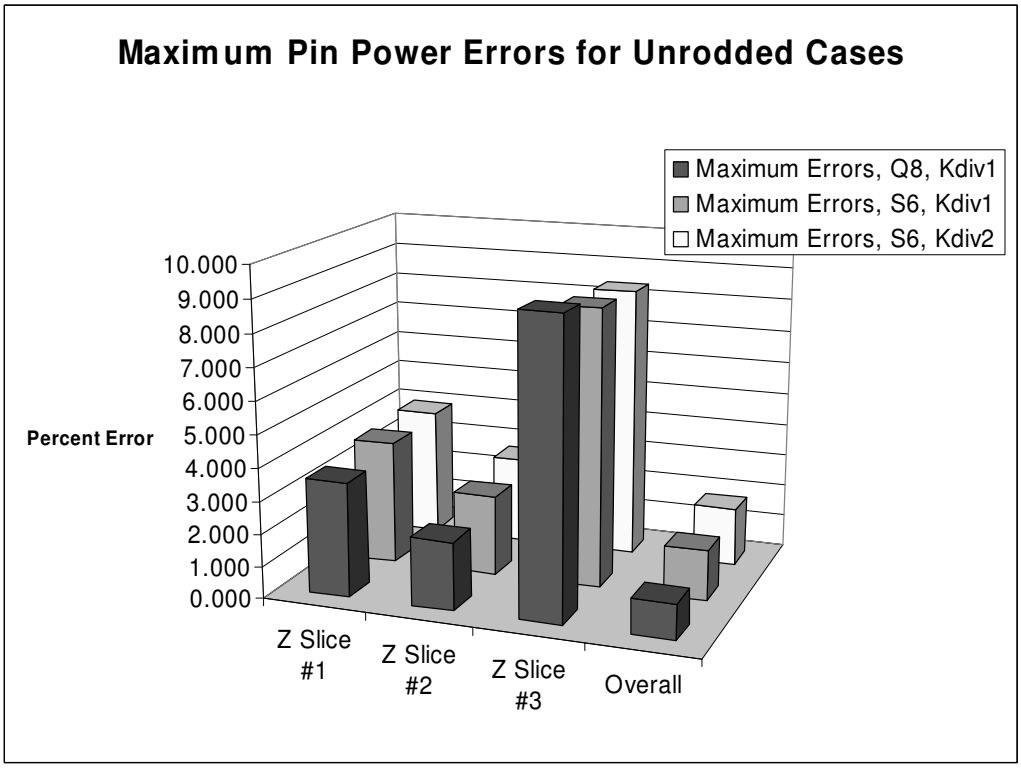

Fig. 10: Maximum Pin Power Errors, Overall and by Slice for the *Unrodded* Case

As the figures show, the differences between all three cases are on the order of a tenth of a percent. It is also apparent that the greatest errors are occurring in slice three. This is the portion of the core that is closest to the control rods in the upper reflector in the *Unrodded* case. The maximum error in the *Unrodded* case is approximately nine percent. For the *Rodded A* and *Rodded B* cases, the maximum error jumps to 33% and 46%, respectively. In the *Rodded B* case, the maximum error in slice two also jumps to approximately 25%. This establishes a fairly clear relationship between increased control rod insertion and increased pin power errors.

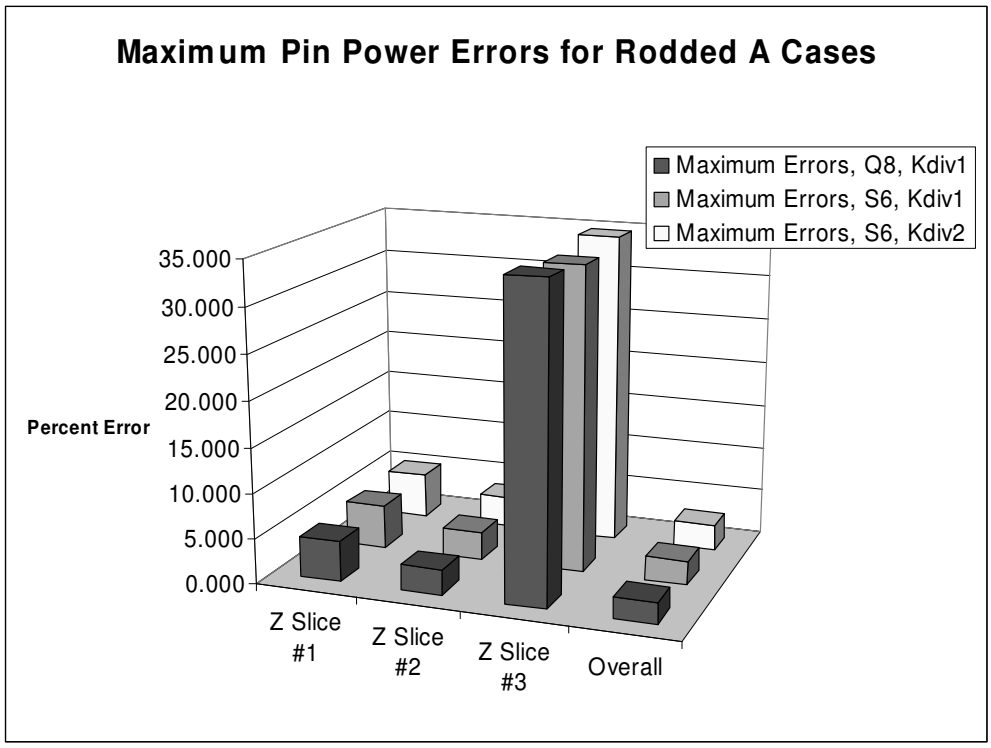

Fig. 11: Maximum Pin Power Errors, Overall and by Slice for the *Rodded A* Case

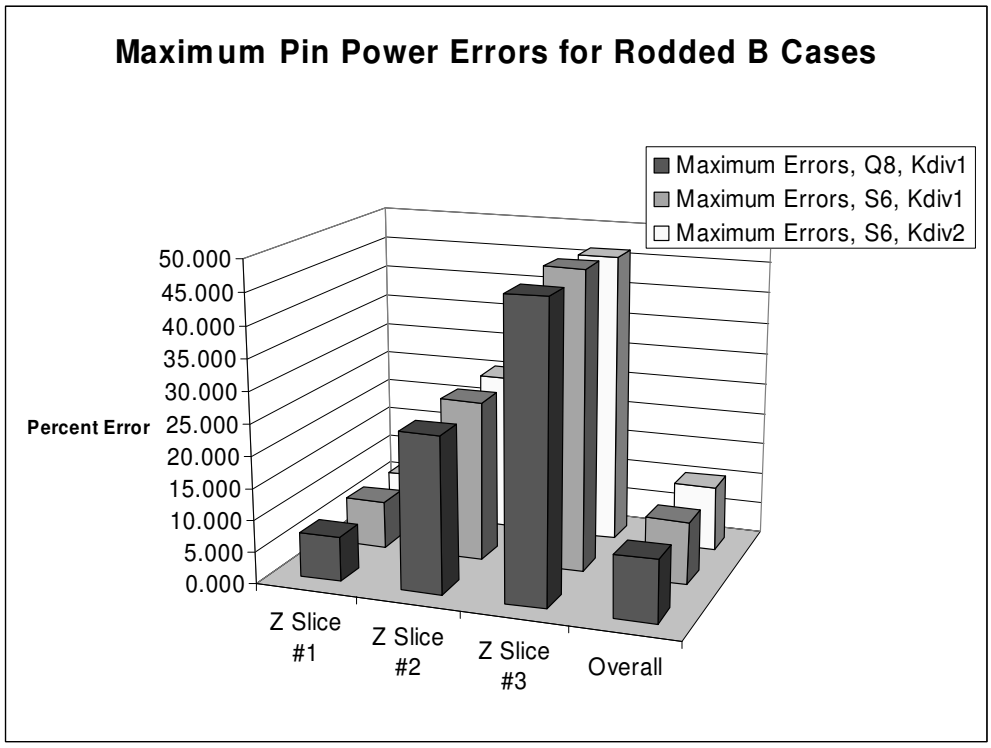

Fig. 12: Maximum Pin Power Errors, Overall and by Slice for the *Rodded B* Case

The notably increased pin power errors in the presence of control rods lead to the final comparison. The axial meshing was changed from the initial 14 cells to 28 cells by dividing each of the computational cells into two. The other attempt was to leave the cells in slice one and two unchanged, while increasing the number of cells in slice two from three to six and increasing the number of cells in the upper reflector from five to 14. The plot of the results for the effective multiplication factor can be seen in Fig. 13.

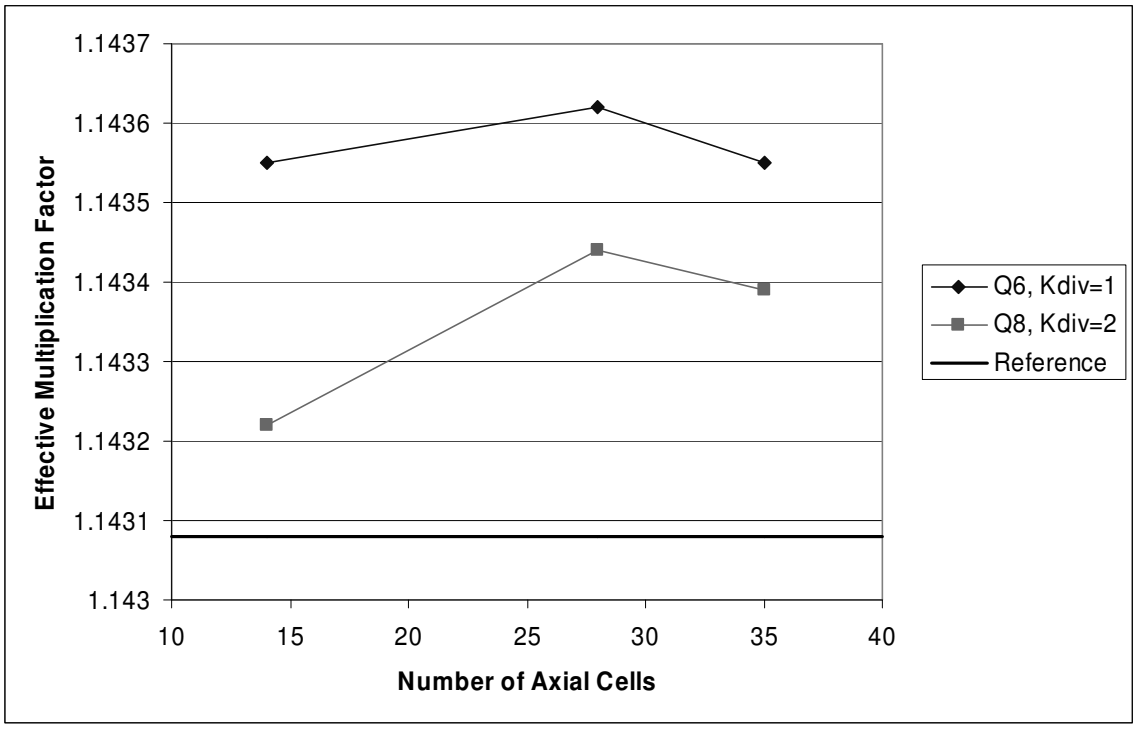

Fig. 13: Effect of Increased Axial Refinement on Infinite Multiplication Factor

The above plot is for the *Unrodded* case only, as the *Rodded A* and *Rodded B* cases gave similar results. There was little significant effect on the pin power errors, so those results are also not shown here.

Conclusions

This benchmark was carried out to test deterministic methods' ability to accurately model heterogeneous reactor systems. As such, the effective multiplication factor and pin powers were the primary criteria for comparison. For the *Unrodded* case, the effective multiplication factor error was always under 0.06% error of the reference value. The concern is that this value did not uniformly converge toward the reference value with increasing mesh refinement or angular quadrature order. This trend was continued in the *Rodded A*, maximum error of 0.17%, and *Rodded B*, maximum error of 0.67%, cases. These errors are actually lower for similar meshes and quadratures than the two-

dimensional benchmark cases. However, in the two-dimensional case simultaneously increasing the angular quadrature order and refining the computational mesh has been shown to lead to convergence of the effective multiplication factor to the reference solution [5]. Computing time prohibits similar quadrature orders from being used in the three-dimensional case.

The pin power errors shown in Figs. 10 through 12 indicate that TORT is giving lower accuracy results in the presence of control elements. This is logical considering the extreme flux gradients that will occur around control elements. Also, the overall pin power errors are much lower than the errors for individual slices. This could be explained by the relatively lower fission rates in the slices containing control elements. The results from the two-dimensional benchmark indicate that increasing the angular quadrature and mesh refinement will alleviate the errors that are exhibited in this case, but a similar setup in three-dimensional geometry would be too computationally expensive to attempt. Also, the three-dimensional results aren't exhibiting the asymptotic behavior that characterized the two-dimensional results. This would lead to the conclusion that some other, at this point unknown, factor is affecting the accuracy of the results.

Acknowledgements

The authors would like to thank Dr. Richard Lillie of Oak Ridge National Laboratory for his guidance into the theory and historical basis behind the DOORS codes, and Oak Ridge National Laboratory (ORNL) and the Oak Ridge Institute for Science Education (ORISE) for providing the necessary equipment and support to allow for this research.

References

1) M. A. Smith, E. E. Lewis, and Byung-Chan Na, "Benchmark on Deterministic 2-D/3-D MOX Fuel Assembly Transport Calculations without Spatial Homogenization: C5G7MOX Benchmark", *NEA/NSC/DOC(2003)16*, March 2003.

2) M. A. Smith, G. Palmiotti, T. A. Taiwo, E. E. Lewis, and N. Tsoulfandis, "Benchmark Specification for Deterministic MOX Fuel Assembly Transport Calculations without Spatial Homogenization (3-D Extension C5G7MOX)", *NEA/NSC/DOC(2003)6*, April 30, 2003.

3) W. A. Rhoades and D. B. Simpson, "The TORT Three-Dimensional Discrete Ordinates Neutron/Photon Transport Code," ORNL/TM-13221, Oak Ridge National Laboratory 1997.

4) R. Orsi, "BOT3P: Bologna Transport Analysis Pre-Post-Processors Version 1.0", Nuclear Science and Engineering, Technical Note, 142, pages 349-354. Nov. 2002.

5) Y. Y. Azmy, J. Gehin, and R. Orsi, "DORT Solutions to Lewis' Two-Dimensional MOX Benchmark Problem", invited for publication in *Progress in Nuclear Energy*.